Journal of Experimental Botany Advance Access published January 20, 2012

*Journal of Experimental Botany*, Page 1 of 9
doi:10.1093/jxb/err445

Journal of Experimental Botany
www.jxb.oxfordjournals.org

RESEARCH PAPER

# MRI links stem water content to stem diameter variations in transpiring trees

**Veerle De Schepper[1,*], Dagmar van Dusschoten[2], Paul Copini[3], Siegfried Jahnke[2] and Kathy Steppe[1]**

[1] Laboratory of Plant Ecology, Department of Applied Ecology and Environmental Biology, Faculty of Bioscience Engineering, Ghent University, Coupure Links 653, 9000 Ghent, Belgium

[2] IBG-2: Plant Sciences, Forschungszentrum Jülich, D-52425 Jülich, Germany

[3] Forest Ecology and Forest Management Group, Centre for Ecosystem Studies, Wageningen University, PO Box 47, 6700AA Wageningen, The Netherlands

* To whom correspondence should be addressed. E-mail: Veerle.DeSchepper@UGent.be

Received 16 June 2011; Revised 12 December 2011; Accepted 14 December 2011

## Abstract

**In trees, stem diameter variations are related to changes in stem water content, because internally stored water is depleted and replenished over a day. To confirm this relationship, non-invasive magnetic resonance imaging (MRI) was combined with point dendrometer measurements in three actively transpiring oak (*Quercus robur* L.) trees. Two of these oak trees were girdled to study the stem increment above the girdling zone. MRI images and micrographs of stem cross-sections revealed a close link between the water distribution and the anatomical features of the stem. Stem tissues with the highest amount of water were physiologically the most active ones, being the youngest differentiating xylem cells, the cambium and the youngest differentiating and conductive phloem cells. Daily changes in stem diameter corresponded well with the simultaneously MRI-measured amount of water, confirming their strong interdependence. MRI images also revealed that the amount of water in the elastic bark tissues, excluding cambium and the youngest phloem, contributed most to the daily stem diameter changes. After bark removal, an additional increase in stem diameter was measured above the girdle. This increase was attributed not only to the cambial production of new cells, but also to swelling of existing bark cells. In conclusion, the comparison of MRI and dendrometer measurements confirmed previous interpretations and applications of dendrometers and illustrates the additional and complementary information MRI can reveal regarding water relations in plants.**

**Key words:** Dendrometer, girdling, LVDT, MRI, micrograph, oak, *Quercus robur* L., stem diameter changes, stem growth, water content, xylem.

## Introduction

Trees are characterized by daily variations in stem diameter (Simonneau *et al.*, 1993; Goldhamer and Fereres, 2004; Steppe *et al.*, 2006; De Schepper *et al.*, 2010). It is hypothesized (Herzog *et al.*, 1995; Steppe and Lemeur, 2004; Steppe *et al.*, 2006; Čermák *et al.*, 2007) that, besides radial growth, these daily diameter variations result from depletion and replenishments of internal stem water reserves caused by a time delay between leaf transpiration and soil water uptake (Schulze *et al.*, 1985; Goldstein *et al.*, 1998; Steppe *et al.*, 2002). This hypothesis is confirmed by many dynamic modelling studies (Génard *et al.*, 2001; Zweifel *et al.*, 2001; Perämäki *et al.*, 2005; Steppe *et al.*, 2006; Steppe *et al.*, 2012), although few experimental measurement attempts have been made to confirm these modelling results in trees (Simonneau *et al.*, 1993; Zweifel *et al.*, 2000). In the past, water content has mostly been measured destructively (Sternberg and Shoshany, 2001), but nowadays accurate *in vivo* measurements on actively transpiring plants are possible due to the application of non-invasive nuclear magnetic resonance (NMR). In the vegetable *Cucumis sativus* L., stem diameter variations corresponded well with dynamics in the amount of stem water measured

by NMR (Reinders *et al.*, 1988). However, to our knowledge, no study so far made this comparison on living trees or tried to quantify the contribution of water from different bark tissues to daily stem diameter variations.

In woody trees, daily stem diameter variations measured over bark are typically much larger than those measured on the xylem (Zweifel *et al.*, 2000). The bark not only contains conductive sieve element–companion cell complexes (SE–CCC), but also many other cell types, such as phloem parenchyma, phloem fibres, cortex, and non-functional, sometimes collapsed, SE–CCC (Trockenbrodt, 1990). A few attempts (Sevanto *et al.*, 2003; De Schepper *et al.*, 2010; Sevanto *et al.*, 2011) have been made to interpret the differences between bark and xylem diameter variations in terms of the interrelated water (xylem) and sugar (phloem) transport. However, to link bark diameter variations to phloem transport correctly, it is important to know the relative contribution of the different bark tissues to the overall bark diameter variation (Sevanto *et al.*, 2011). A relatively low contribution of 15 % of cambium and conductive SE–CCC to the overall bark diameter variation has been suggested by De Schepper and Steppe (2010).

Tree girdling is often applied to study carbon transport (Williams *et al.*, 2000; De Schepper *et al.*, 2010; De Schepper and Steppe, 2011). The stem diameter above a girdling typically increases due to growth of bark and xylem, stimulated by the accumulation of carbohydrates (Daudet *et al.*, 2005; De Schepper *et al.*, 2010). *In vivo* stem water content measurements can verify whether the stem diameter increase results from cambial production of new cells and swelling of existing cells, as suggested by De Schepper *et al.* (2010).

The imaging branch of NMR, magnetic resonance imaging (MRI), can estimate *in vivo* the amount of water in tree stems (Van As, 2007; Merela *et al.*, 2009*a*) and allows differentiation between different stem tissues (Van As *et al.*, 2009). MRI was therefore applied in our study to verify the above hypotheses. As such, the main objectives of this study were: (i) to evaluate the direct link between stem diameter variations and stem water content in living trees; (ii) to investigate how changes in water content of different bark tissues contribute to overall stem diameter variations; and (ii) to verify whether the stem increment above the girdle is due to the production of new cells and/or swelling of existing cells.

## Materials and methods

### *Plant material and experimental set-up*

Measurements were conducted on three 2-year-old oak trees (*Quercus robur* L.) with a stem diameter of 1.4±0.1 cm and a height of 112±3 cm. On 15 March 2010, the trees, previously grown in an outdoor tree nursery, were replanted in 10 l containers. The containers were filled with a potting mixture (LP502D, Peltracom nv, Belgium) and fertilized with a slow releasing NPK plus magnesium mix (Basacote Plus 6M, COMP0, Benelux). The potting mixture remained well humidified as the trees were watered every 2–3 d. The first tree was a control tree without bark manipulation. A strip of bark of the second tree was removed along the complete outer circumference (fully girdled tree), whereas a strip of bark was only removed along half of the outer circumference of the third tree (half-girdled tree). MRI and dendrometer measurements were simultaneously performed for several days in October [control tree: day of year (DOY) 286–287; fully girdled tree: DOY 280–283; half-girdled tree: 288–290]. The fully girdled and half-girdled trees were girdled 2–3 d prior to the measurements, namely at DOY 277 and DOY 286, respectively. The strips of bark removed were approximately 1 cm wide and carefully detached from the xylem at a height of approximately 40 cm above the soil surface. Stem segments were harvested to make stem micrographs. The samples of the fully girdled tree were taken 16 d (DOY 293) after girdling.

### *MRI-derived amount of stem water*

The oak trees were placed one at a time in an MRI system at Forschungszentrum Jülich (IBG-2, Plant Sciences), each tree for several days. A 1.5T MRI system was used consisting of a split-coil magnet (Magnex/Agilent, Oxford, UK) and an NMR imaging spectrometer (Varian/Agilent, Alto Palo, USA). The split between the magnet halves is 50 cm. A ditch with an elevator system below the split allowed insertion of the trees. To increase the transpiration of the control tree, dry air was blown in the close vicinity of the leaves.

For imaging purposes, parallel magnetic field gradient-inserts at a separation of 120 mm were used (plate diameter 40 cm, gradient strength up to 800 mT $m^{-1}$). In between these two inserts a part of the oak stem was placed. A small solenoid radio-frequency (RF) coil was wound around the stem prior to measurements. This resulted in a small RF coil which yielded a much higher signal-to-noise ratio with respect to a standard whole body RF coil. Images were acquired using (multiple) spin echoes, which are much less sensitive to magnetic field deviations that may occur due to air pockets in the stem compared to gradient echoes (Haacke *et al.*, 1999). Echo times were minimized to 5.4 ms which reduces $T_2$ effects, so the first echo images were a good approximation of the amount of water. The amount of water per pixel within the tree can be calibrated by means of a signal intensity comparison with a reference tube placed directly against the tree. Spin echo trains, consisting of at least 16 spin echoes, were acquired to monitor $T_2$ in order to be able to correct for changes in this relaxation process over time. This train of echoes was fitted to a mono-exponential curve which yields a $T_2$ time and the 'true' amount of water on a pixel-by-pixel basis. The single-exponential function resulted in a reproducibility of 1–2% for water-rich regions. Even though the reproducibility is high for MRI standards, the single-exponential fits could only be used for verification purposes. In a 1.5T-MRI system, the $T_2$ is predominantly influenced by the cell size (especially the vacuole) and to a lesser extent by the membrane permeability (Van As, 2007) and the thickness of the cell walls relative to the cell size. Small $T_2$ changes over time were observed but could not be linked to amplitude changes. Therefore, using the first echo image intensities was a good approximation for the amount of water per pixel. In addition, multi-echo experiments were performed with a set of reduced repetition times to be able to also determine $T_1$ in order to explain MRI contrast, in relation to tissue properties (e.g. amount of water or cell size). During all measurements, a slice thickness of 2.5 mm was used with a fixed in-plane resolution (pixel size) of 100 μm. Due to this fixed resolution, the field of view varied between 18 mm and 20 mm. Using custom-made fitting routines, the experiments were fitted to:

$$S(TE, TR) = \left(1 - e^{(-\mathrm{TR}/\mathrm{T1})}\right) e^{(-\mathrm{TE}/\mathrm{T2})} \rho$$

where $S$ is the signal intensity, $TE$ represents the echo time(s), $TR$ is the repetition time(s), and ρ is the spin density (~amount of water per pixel). All data analysis routines, from image reconstruction to fitting, were written in IDL (ITT, Boulder, USA), a high level command line language.

### *Microclimatic measurements*

Within the 1.5T-MRI magnet, the photosynthetic active radiation (PAR) was provided by a MIG spotlight (LEG Illumination, Milan, Italy) with a 400 W HQI daylight lamp (Radium, Wipperfürth, Germany) placed to one side of the MRI-magnet. The light beam was mainly directed on the leaves at one side of the tree. During the MRI measurements, a PAR-sensor (Li-190S, Li-Cor, Lincoln, NE, USA) continuously measured the amount of PAR that the crown received on the illuminated side. To achieve a stable MRI measurement, the air in the 1.5T-MRI setup was controlled at a constant temperature of 21±1 °C. In addition, continuous ventilation took place in the set-up. Air temperature (measured by a copper–constantan thermocouple, Omega, Amstelveen, The Netherlands) and relative air humidity (measured by a Hygroclip S, Rotronic, AG Schweiz, Bassersdorf, Switzerland) were measured in the middle of the tree crown and used to calculate the vapour pressure deficit of the air (VPD). VPD is defined as the difference between the saturation pressure at air temperature and ambient vapour pressure (Jones, 1992).

### *Stem diameter measurements*

Variations in stem diameter were continuously measured with a specific type of point dendrometer: linear motion potentiometer (LP-20F-6, Natkon, Hombrechtikon, Switzerland). Other types of point dendrometers (e.g. linear variable displacement transducers or LVDTs) of which the measurement principle is based on magnetic coils could not be used in this application, because the strong magnetic interferes with their proper operation. The dendrometer was supported by a custom-made stainless-steel frame that does not require a temperature correction (Steppe and Lemeur, 2004). The dendrometer was installed on the main stem above and as close as possible to the RF coil, allowing a distance of at least 20 cm between both to avoid possible interference between the magnetic field and the electrical wires connecting the dendrometer with the datalogger. All sensor signals (microclimate and dendrometers) were logged at 10 s intervals and 5 min means were stored using a data logger (DL2, Solartron Metrology, Leicester, England).

### *Stem anatomy*

Stem micrographs were made of the control and the fully girdled tree. Stem segments of about 10 cm long, including the 2.5 mm slice scanned by MRI, were sampled and stored in a 50% ethanol solution at ambient room temperature. Cross-sections with a thickness of about 25 μm were cut from the stem segments using a sliding microtome (G.S.L.-1 microtome, WSL, Birmensdorf, Switzerland). The segments of the girdled tree were sampled at three positions: 0.5 cm above the girdle, the girdle itself, and 1 cm below. All cross-sections were stained with a safranine/astrablue solution for 5 min. Following dehydration in graded series of ethanol (50–95–100%), the samples were rinsed with xylol, mounted in Canada balsam and dried at 60 °C for 15 h. Photographs were taken with a digital camera (DFC 320, Leica, Cambridge, UK) mounted on a microscope (DM2500, Leica, Cambridge, UK) using Leica imaging software (version 3.6.0).

## Results

### *Link between MRI images and stem anatomy*

An optical stem micrograph (Fig. 1A, B) of the control tree shows the typical anatomical features of an oak stem (Trockenbrodt, 1991). The red colour indicates lignified cells such as xylem vessels, phloem and xylem fibres or sclereids; the blue colour indicates non-lignified cells such as parenchyma, SE–CCC and differentiating cells. Figure 1C shows an MRI image with reduced $T_2$-weighing of a 2.5 mm slice close to the section of the micrograph of Fig. 1A, B: white represents a high amount of water per pixel and dark grey represents a low amount of water per pixel. Early and late wood vessels contained much more water than the xylem fibres which are almost black (Fig. 1C). The bright white band with a high amount of water (up to 95%) contained not only the cambium but also the youngest secondary phloem and xylem (Fig. 1D). The amount of water of the remaining bark was rather low (between 20% and 40%). Note that the amount of water in the pith was also low.

The location of the cambium cells in the white zone (Fig. 2B) shows up as an intermediate $T_2$ (50–60 ms) and a dark $T_1$ (around 200 ms) band (arrow Fig. 2A, C). The lignified part of the wood is relatively bright in the $T_1$ image since lignin has much less exchangeable protons than cellulose which causes an increased $T_1$ (up to 800 ms). The bright zones in the $T_2$ image ($T_2$ values of about 120 ms) represent water-filled xylem vessels that are relatively large and therefore attenuation of $T_2$ is small.

### *Link between stem diameter variations and amount of stem water*

Natural environmental conditions were mimicked in the MRI setup (Fig. 3). The imposed PAR (about 400 μmol $m^{-2}$ $s^{-1}$) was quite low, but mimicked light conditions that oak seedlings might experience at the forest floor (Clinton, 2003). Because PAR-dynamics and VPD influence the onset and ending of transpiration and the magnitude of transpiration, respectively, they are both indirectly responsible for shrinkage and swelling of the stem (Fig. 4). VPD differed among the different experiments (Fig. 3) as the air temperature in the MRI set-up was controlled with outside air of which the relative humidity fluctuated.

Stem diameter variations correlated well with the normalized amount of water in the stem (Fig. 4). Because this amount of water was integrated across the stem cross-section, the second power of the normalized stem diameter variations was used for comparison. The magnitudes of transpiration-induced decreases and increases in both the stem diameter and the amount of stem water were similar. While radial stem growth was negligible in the control tree (Fig. 4A), growth was detected above the full girdle, although the increase was smaller compared to the increase in amount of water (Fig. 4B). A similar but less pronounced effect was observed in the half-girdled tree (Fig. 4C).

### *Different stem tissues contribute differently to daily swelling and shrinkage*

Figure 5A shows the change in the amount of water between a dark (24.00 h DOY 286) and light (14.00 h DOY 286) period for the control tree. Grey colours identical to that of the background denote no change in the amount of water; whereas lighter and darker colours indicate an

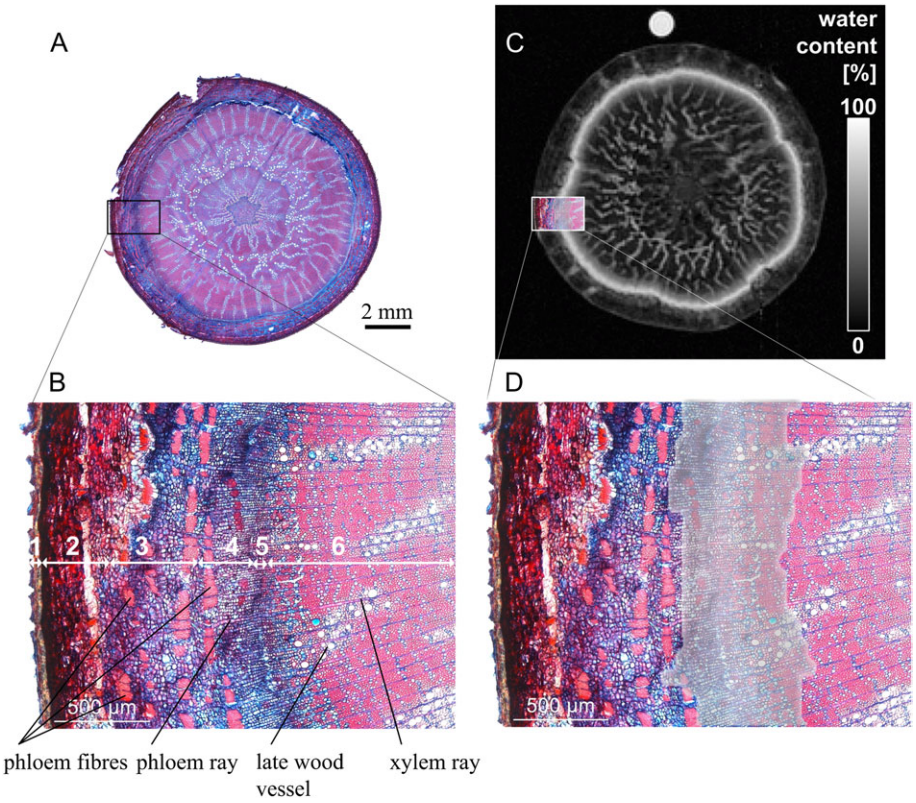


**Fig. 1.** (A) A micrograph of a stem cross-section of an oak tree and (B) a detail of it showing anatomical features: 1, periderm; 2, cortex; 3, dilatated phloem; 4, non-dilatated phloem; 5, cambial zone; 6, xylem; the tissues denoted 1–4 make up the bark and tissue 6 the wood. (C) The amount of water in a similar stem cross-section measured by MRI, (D) partially overlaid with the detailed micrograph to illustrate the position of the white MRI band (indicating a zone with a high amount of water) in relation to anatomical features.

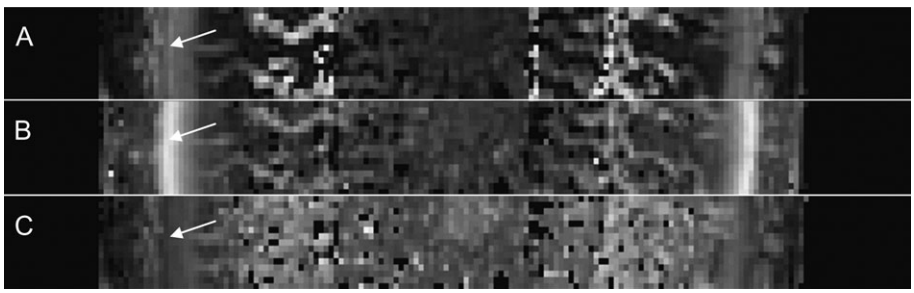


**Fig. 2.** A part of the stem cross-section along the diameter visualized with different MRI images: (A) a $T_2$-image, (B) an image of the amount of water and (C) a $T_1$-image. The maximum range (white) for $T_2$ is 120 ms and for $T_1$ 800 ms. Comparison of these three images indicates a high density of small cells (white arrow) within the zone of a high amount of water (white colour).

increase and a decrease in the amount of water with time, respectively. The outer edge of the difference-image (Fig. 5A) was almost entirely white indicating stem growth during the two measurements as air adjacent to the stem was replaced by newly formed tissue. Furthermore, the bark region was lighter than the background indicating that the amount of water in the bark increased between 14.00 h and 24.00 h. The bright zone (Fig. 1C) was darker on the inside and brighter on the outside compared with the background (Fig. 5A), indicating that the cambial zone was pushed outwards due to cambial production of new cells. It appears that the amount of water in the xylem did not differ a lot between the light and dark periods, as its signal intensity was close to the background intensity (Fig. 5A). Still, the slightly darker colour of the xylem tissue indicates a build-up of cell walls, thereby reducing the amount of water in this zone. On the right-hand side of Fig. 5A, the image displays two noise lines caused by the dendrometer and microclimatic sensors into the MRI set-up.

To quantify the contribution of the different stem tissues due to the transpiration-induced stem diameter changes, a mask was defined which divided the stem into three different zones (Fig. 5B). The mask indicated in orange was equal to the initial zone with a high amount of water (Fig. 1C) and defines three zones: (1) a zone outside the mask containing almost the entire bark; (2) the mask itself

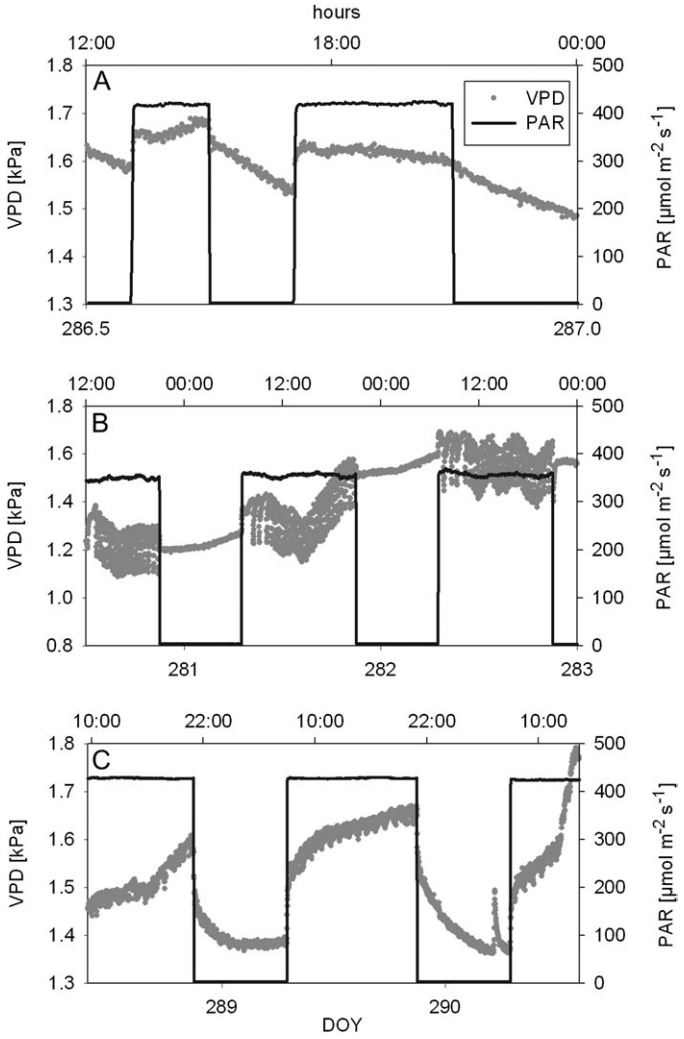


**Fig. 3.** The microclimatic conditions [vapour pressure deficit (VPD) and photosynthetic active radiation (PAR)] in the MRI setup during measurement of (A) the control tree, (B) the fully girdled tree, and (C) the half-girdled tree. DOY, day of the year.

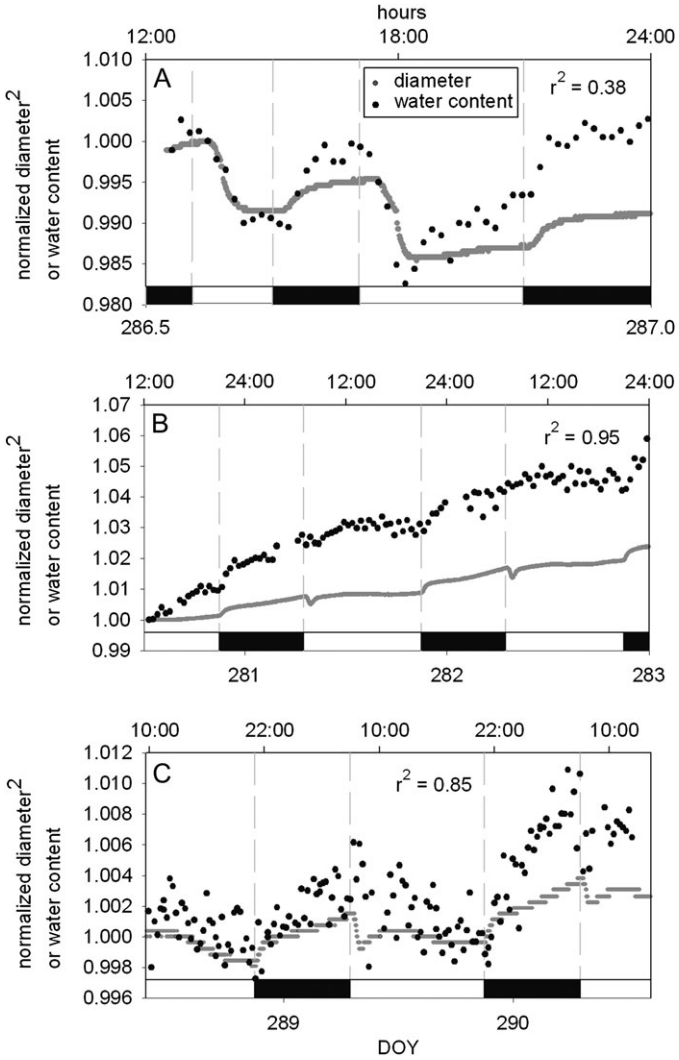


**Fig. 4.** Dynamics of the stem diameter measured with a dendrometer and the MRI derived amount of water for (A) the control tree, (B) the fully girdled tree, and (C) the half-girdled tree. The stem diameter and amount of water were normalized by dividing them with their initial value, the second power of the normalized stem diameter is used to scale them to the same dimensions of the amount of water. $r^2$ is the determination coefficient which informs about the correlation between LVDT and MRI measurements. Black boxes indicate night periods, DOY, day of the year.

containing the cambium, youngest phloem and xylem; and (3) a zone inside the mask containing the xylem. The mask and the three zones are defined based on the first measured MRI-image (12 00 h DOY 286). Due to the current status of image-processing, the mask could not be made dynamic in time. Figure 5C illustrates the changes in time of the amount of water in the defined stem zones. The bark (zone 1) was losing the highest amount of water during the transpiration-induced shrinkages, while the xylem (zone 3) did barely contribute to the total water loss. The zone with the highest amount of water (zone 2) contributed significantly less compared to zone 1. Note that, as time evolved and especially towards the end of the measurement period, the amount of bark water increased, while it decreased in the xylem. This behaviour is attributed to the fixed position of the mask whereas, in reality, the mask should move outward with time due to cambial production. Therefore, the contributions estimated in Table 1 are based on the first period of water loss (Fig. 5C). The maximum water loss relative to the amount of water in the zone itself was much higher in zone 1 (bark) compared with the other two zones. Assuming that the entire bark consisted of zone 1 and half of zone 2, the contribution of water from the bark to the total water loss in the stem was 71.5%, whereas the xylem contribution (zone 3 and other half of zone 2) was only 28.5%. Based on the same assumption we estimated that the cambium and youngest phloem (half of zone 2) contributed 13.5% to the total bark diameter variations.

### *Stem increment above the full girdle*

The stem increment in time above the full girdle is depicted in Fig. 6A. The positioning of this pixel row is roughly indicated by arrow 'd' in Fig. 6B. Stem growth over 88 h was about two

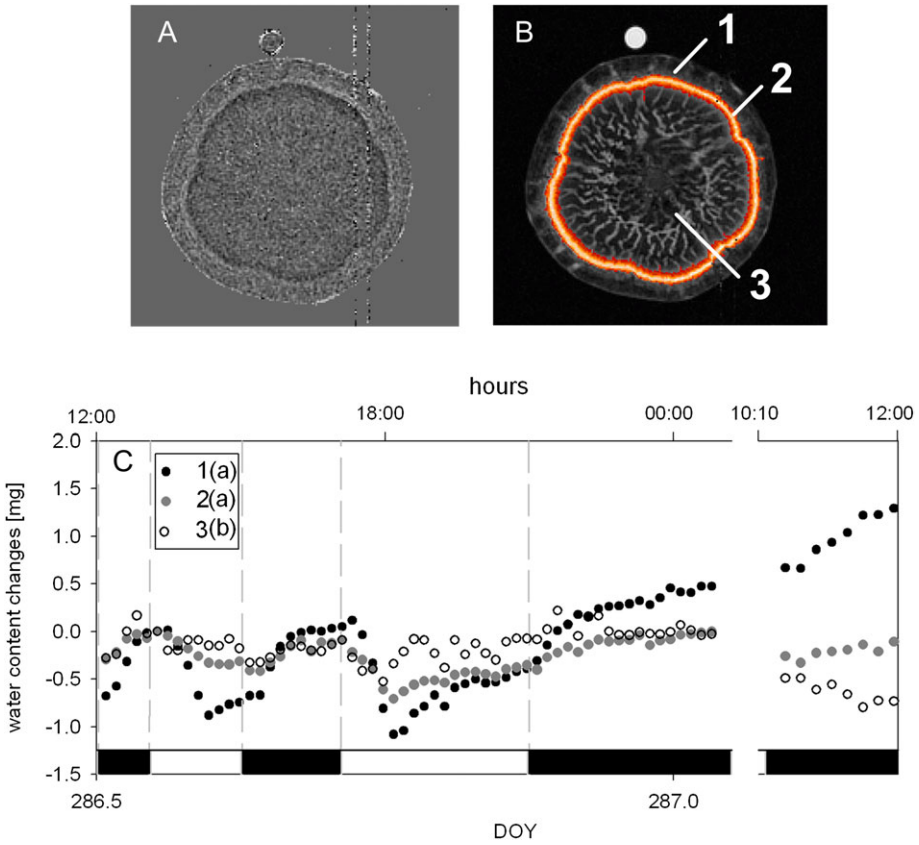


**Fig. 5.** (A) The difference in the amount of water between the stem cross-section of the control tree taken during the dark period at 24.00 h DOY 286 and the stem cross-section taken during the light period at 14.00 h DOY 286, (B) the amount of water in the stem cross-section at the beginning of the measurements with the selected mask in orange that covers the band with a high amount of water (white). Based on this mask three distinct zone are defined: (1) zone 1 is located outside the mask, (2) zone 2 is the mask itself (orange band), and (3) zone 3 is located inside the mask; (C) the time dynamics of the amount of water in the three zones, note that the time axis is interrupted for a few hours during DOY 287. Different letters in the legend indicate a significant difference (Tuckey, $P \leqslant 0.05$) of the overall mean of all shown data points. Black boxes indicate night periods, DOY, day of the year.

**Table 1.** Maximum water loss relative to its original amount of water per stem zone (%) and the average contribution of the stem zone to the total water loss in the stem based on the first shrink of the control tree at 14 00 h DOY 286 in Fig. 5. The stem zones were defined as depicted in Fig. 5B; here, the main tissues of the different zones are stated in parentheses.

| Stem zone | Maximum water loss relative to the original amount of water in the zone (%) | Average water loss relative to the total water loss in the stem (%) |
|---|---|---|
| Zone 1 (bark) | 3.3 | 58 |
| Zone 2 (cambium) | 0.9 | 27 |
| Zone 3 (wood) | 0.2 | 15 |

pixels (~200 μm). The displacement of the bright zone indicates that both xylem and phloem have grown close to one pixel (~100 μm) at the right and left side, respectively (Fig. 6A). As such, the time sequence confirmed that the zone with the highest amount of water contained the cambium. The xylem and bark growth were also visible in stem micrographs sampled above the girdle 16 d after girdling (Fig. 6B). The tree reacted above (Fig. 6B) and at the girdle (Fig. 6C) by the production of many differentiating non-lignified cells (blue) which contained a band of lignifying small xylem vessels and tracheids (red) (arrow 'a') and a distinct band of phloem fibres (red) (arrow 'b'). These girdling responses were not observed below the girdle (Fig. 6D). Based on both distinct features and the positioning of the cambium (black point), the growth of new stem tissue above the girdle (arrow 'c' in Fig. 6B) could be estimated. The growth of phloem tissue (378±48 μm), was significantly larger (Student's $t$ test, $P$ <0.05) than that of xylem (326±65 μm) 16 d after girdling. If growth happened linearly, the phloem and xylem growth rates estimated from MRI (phloem: 25 μm $d^{-1}$; xylem: 25 μm $d^{-1}$) and micrographs (phloem: 24 μm $d^{-1}$; xylem: 20 μm $d^{-1}$) were quite similar. A similar but less pronounced growth took place at the girdle itself (Fig. 6C).

In addition, changes in the amount of bark water were evaluated over time. A mask of the bark of the fully girdled tree was made at the beginning and at the end of the measurement period (two days) in similar dark conditions. Comparison of the amount of water in both masks revealed that the mean amount of water per pixel had increased with 25±5%.

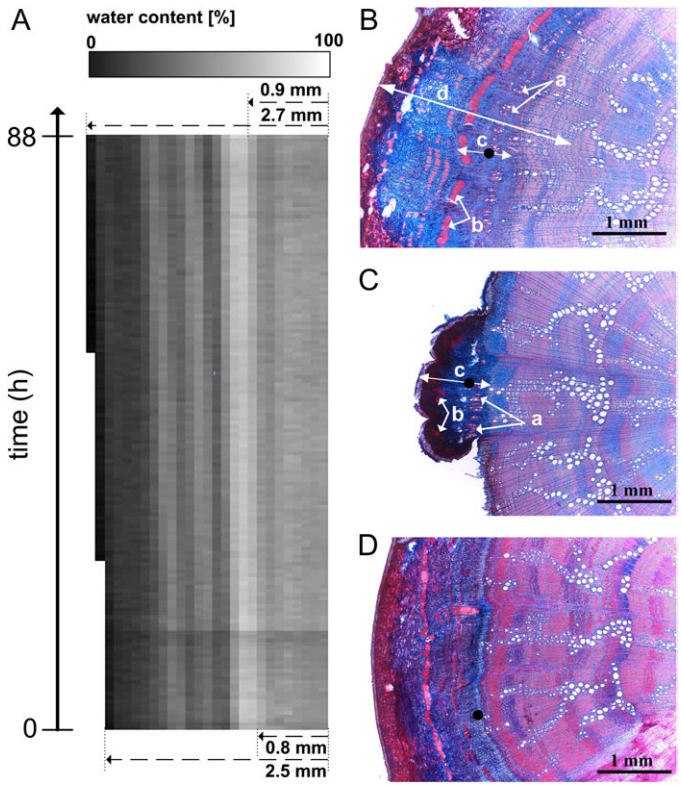


**Fig. 6.** Girdling responses of the stem after full girdling illustrated with MRI images and anatomical micrographs. (A) The same pixel row taken from a series of images showing the amount of water in the same stem cross-section measured above the full girdle and taken on subsequent times. The pixel row of the earliest measurement is shown at the bottom and the latest measurement at the top. The pixel row covers more or less the stem width indicated by arrow 'd' in Fig. 6B. The two dashed arrows represent the width of the xylem tissue in the pixel row (changing from 0.8–0.9 mm with time) and the width of the total pixel row (2.5–2.7 mm). Anatomical cross-section of the stem sampled 16 d after girdling: (B) above the girdling zone, (C) at the girdling zone; and (D) below the girdling zone. Arrow 'a' indicates newly formed xylem vessels in between undifferentiated xylem cells, arrow 'b' indicates phloem fibres massively formed after girdling; and arrow 'c' indicates the stem tissue formed after girdling, the black dot represents the current position of the cambium.

## Discussion

### *Most physiologically active stem tissues have the highest water content*

It is likely that the zone with the highest amount of water (white band in Fig. 1C) is the most physiologically active one because it also contains, besides the cambium and differentiating xylem and phloem cells, conductive sieve tubes. MRI-flow measurements on poplar have indeed shown that conductive sieve tubes are located within the zone with the highest amount of water (Windt *et al.*, 2006) and it is generally accepted that only the current year's growth increment of phloem is active in long-distance sugar transport through the stem (Raven *et al.*, 1999; Rosner *et al.*, 2001). The high amount of water in this zone can be attributed to the large water retention by the osmotically active substances in the conductive sieve tubes (Rosner *et al.*, 2001; Thompson, 2006).

### *Stem diameter variations are related to changes in stem water content*

The strong correlation between transpiration-induced changes in stem diameter and the amount of stem water (Fig. 4) proves the value of stem diameter variations for estimating the *in vivo* use of internally stored water. The difference in increase between stem diameter and the amount of water can partially be explained by the fact that growth is not only an increase in the amount of cell water but also in cell density. Secondly, a point dendrometer measures changes in stem diameter based on several contact points with the bark, whereas MRI measures the entire stem cross-section. Particularly in this MRI set-up, with illumination on one side, asymmetrical stem growth could cause a stem diameter measurement to be less representative for the entire cross-section. Thirdly, the disparity could result from the different distance of both measurement locations to the girdle, with the point dendrometer farther away diminishing radial stem growth (De Schepper *et al.*, 2010). Lastly, it is possible that tissue water, which was initially invisible for MRI ($T_2$ less than 2 ms), became visible (increase in its $T_2$ value).

### *Elastic bark contributes most to stem diameter variations*

The amount of water measured *in vivo* (Fig. 5; Table 1) confirms the hypothesis that changes in stem diameter are mainly caused by changes in bark water content (Irvine and Grace, 1997; Zweifel *et al.*, 2001; Hölttä *et al.*, 2006; Steppe *et al.*, 2006; De Schepper and Steppe, 2010; Steppe *et al.*, 2012). It is striking that the bark tissues with the highest amount of water (i.e. the cambium and the youngest differentiating and conductive phloem) do not contribute most to stem diameter shrinkage. The lower contribution of these tissues (13.5%, comparable to the modelled 15% of De Schepper and Steppe, 2010) can be expected, because the high concentrations of osmotically active substances in the cambium and conductive phloem retain water very effectively. The less physiologically active (cf. non-conductive phloem tissue) bark cells contributed most to the stem's water storage capacity.

### *Tissue production and swelling above a girdle*

Other girdling experiments (Noel, 1970; Aloni and Zimmermann, 1984) reported a similar production of lignified xylem vessels and tracheids (arrow 'a' in Fig. 6B, C) located in a zone of non-lignified differentiating cells. The production of multiple phloem fibres (arrow 'b' in Fig. 6B, C) in the bark was also observed in beech after wounding (Merela *et al.*, 2009*b*).

The increased amount of water in the bark after girdling confirms that the stem increase is not only attributed to the production of new cells but also to swelling of existing cells. Merela *et al.* (2009*b*) reported a similar increase in the amount of water after wounding in beech. This swelling effect probably results from an increased concentration of osmotic active substances such as sugars (De Schepper *et al.*, 2010) and potassium (Merela *et al.*, 2009*b*).

## Conclusions

The strong correspondence between stem diameter variations and changes in the amount of stem water, both simultaneously measured *in vivo* in young oaks, confirms their direct link. Based on time lags in water transport, this link has been amply suggested in the literature and already used in mechanistic modelling studies. Our MRI measurements indicate that the elastic bark tissues, without the young conductive phloem or cambium tissues, contribute most to the daily depletion of internal stem water storages. Stem diameter variations are hence mainly driven by changes in the amount of water in these elastic bark tissues. Following girdling, the stem increase observed above the girdle was due to the production of new cells and swelling of existing cells. The latter is probably due to an accumulation of osmotic active substances in the bark cells. The use and interpretation of continuous dendrometer measurements is validated with MRI on oak trees, which, in addition, can provide complementary information about the amount of water and its distribution in plant stems.

## Acknowledgements

We are indebted to Johannes Kochs of the NMR group at IBG-2 (Forschungszentrum Jülich) and to Philip Deman and Geert Favyts of the Laboratory of Plant Ecology (UGent) for their accurate and enthusiastic technical support. We thank the Research Foundation—Flanders (FWO) for the PhD funding granted to Veerle De Schepper and the scientific research committee (CWO) of the Faculty of bioscience engineering (UGent) to support the research visit of Veerle De Schepper at the Forschungszentrum Jülich.

## References

**Aloni R, Zimmermann MH.** 1984. Length, width, and pattern of regenerative vessels along strips of vascular tissue. *Botanical Gazette* **145,** 50–54.

**Čermák J, Kučera J, Bauerle WL, Phillips N, Hinckley TM.** 2007. Tree water storage and its diurnal dynamics related to sap flow and changes in stem volume in old-growth Douglas-fir trees. *Tree Physiology* **27,** 181–198.

**Clinton BD.** 2003. Light, temperature, and soil moisture responses to elevation, evergreen understory, and small, canopy gaps in the southern Appalachians. *Forest Ecology and Management* **186,** 243–255.

**Daudet FA, Améglio T, Cochard H, Archilla O, Lacointe A.** 2005. Experimental analysis of the role of water and carbon in tree stem diameter variations. *Journal of Experimental Botany* **56,** 135–144.

**De Schepper V, Steppe K.** 2010. Development and verification of a water and sugar transport model using measured stem diameter variations. *Journal of Experimental Botany* **61,** 2083–2099.

**De Schepper V, Steppe K.** 2011. Tree girdling responses simulated by a carbon and water transport model. *Annals of Botany* (in press).

**De Schepper V, Steppe K, Van Labeke MC, Lemeur R.** 2010. Detailed analysis of double girdling effects on stem diameter variations and sap flow in young oak trees. *Environmental and Experimental Botany* **68,** 149–156.

**Génard M, Fishman S, Vercambre G, Huguet J-G, Bussi C, Besset J, Habib R.** 2001. A biophysical analysis of stem and root diameter variations in woody plants. *Plant Physiology* **126,** 188–202.

**Goldhamer DA, Fereres E.** 2004. Irrigation scheduling of almond trees with trunk diameter sensors. *Irrigation Science* **23,** 11–19.

**Goldstein G, Andrade JL, Meinzer FC, Holbrook NM, Cavelier J, Jackson P, Celis A.** 1998. Stem water storage and diurnal patterns of water use in tropical forest canopy trees. *Plant, Cell and Environment* **21,** 397–406.

**Haacke EM, Venkatesan R, Wang Y, Yu Y.** 1999. Three dimensional gradient echo imaging. In: Naruse S, Watari H, eds. *Proceedings of the international symposium on ultrafast magnetic resonance imaging in medicine*. Kyoto, Japan: Elsevier Science, 39–47.

**Herzog KM, Häsler R, Thum R.** 1995. Diurnal changes in the radius of sub-alpine Norway Spruce stem: their relation to the sap flow and their use to estimate transpiration. *Trees–Structure and Function* **10,** 94–101.

**Hölttä T, Vesala T, Sevanto S, Perämäki M, Nikinmaa E.** 2006. Modeling xylem and phloem water flows in trees according to cohesion theory and Münch hypothesis. *Trees* **20,** 67–78.

**Irvine J, Grace J.** 1997. Continuous measurements of water tensions in the xylem of trees based on the elastic properties of wood. *Planta* **202,** 455–461.

**Jones HG.** 1992. *Plants and microclimate, a quantitative approach to environmental plant physiology*, 2nd edn. Cambridge: Cambridge University Press.

**Merela M, Oven P, Serša I, Mikac U.** 2009*a*. A single point NMR method for an instantaneous determination of the moisture content of wood. *Holzforschung* **63,** 348–351.

**Merela M, Pelicon P, Vavpetič P, Regvar M, Vogel-Mikuš K, Serša I, Poličnik H, Pokorny B, Levanič T, Oven P.** 2009*b*. Application of micro-PIXE, MRI and light microscopy for research in wood science and dendroecology. *Nuclear Instruments and Methods in Physics Research Section B-Beam Interactions with Materials and Atoms* **267,** 2157–2162.

**Noel ARA.** 1970. The girdled tree. *Botanical Reviews* **36,** 162–195.

**Perämäki M, Vesala T, Nikinmaa E.** 2005. Modeling the dynamics of pressure propagation and diameter variation in tree sapwood. *Tree Physiology* **25,** 1091–1099.

**Raven PH, Evert RE, Eichhorn SE.** 1999. *Biology of plants*, 6th edn. New York: Worth Publishers.

**Reinders JEA, Vanas H, Schaafsma TJ, Sheriff DW.** 1988. Water-balance in *Cucumis* plants measured by nuclear magnetic-resonance. 2. *Journal of Experimental Botany* **39,** 1211–1220.

**Rosner S, Baier P, Kikuta SB.** 2001. Osmotic potential of Norway spruce [*Picea abies* (L.) Karst.] secondary phloem in relation to anatomy. *Trees–Structure and Function* **15,** 472–482.

**Schulze ED, Čermák J, Matyssek R, Penka M, Zimmermann R, Vasicek F, Gries W, Kučera J.** 1985. Canopy transpiration and water fluxes in the xylem of the trunk of *Larix* and *Picea* trees: a comparison of xylem flow, porometer and cuvette measurements. *Oecologia* **66,** 475–483.

**Sevanto S, Hölttä T, Holbrook NM.** 2011. Effects of the hydraulic coupling between xylem and phloem on diurnal phloem diameter variation. *Plant, Cell and Environment* **34,** 690–703.

**Sevanto S, Vesala T, Peramaki M, Nikinmaa E.** 2003. Sugar transport together with environmental conditions controls time lags between xylem and stem diameter changes. *Plant, Cell and Environment* **26,** 1257–1265.

**Simonneau T, Habib R, Goutouly JP, Huguet JG.** 1993. Diurnal changes in stem diameter depend upon variations in water-content - direct evidence in peach-trees. *Journal of Experimental Botany* **44,** 615–621.

**Steppe K, Cochard H, Lacointe A, Améglio T.** 2012. Could rapid diameter changes be facilitated by a variable hydraulic conductance? *Plant, Cell and Environment* **35,** 150–157.

**Steppe K, De Pauw DJW, Lemeur R, Vanrolleghem PA.** 2006. A mathematical model linking tree sap flow dynamics to daily stem diameter fluctuations and radial stem growth. *Tree Physiology* **26,** 257–273.

**Steppe K, Lemeur R.** 2004. An experimental system for analysis of the dynamic sap-flow characteristics in young trees: results of a beech tree. *Functional Plant Biology* **31,** 83–92.

**Steppe K, Lemeur R, Samson R.** 2002. Sap flow dynamics of a beech tree during the solar eclipse of 11 August 1999. *Agricultural and Forest Meteorology* **112,** 139–149.

**Sternberg M, Shoshany M.** 2001. Aboveground biomass allocation and water content relationships in Mediterranean trees and shrubs in two climatological regions in Israel. *Plant Ecology* **157,** 171–179.

**Thompson MV.** 2006. Phloem: the long and the short of it. *Trends in Plant Science* **11,** 26–32.

**Trockenbrodt M.** 1990. Survey and discussion of the terminology used in bark anatomy. *Iawa Bulletin* **11,** 141–166.

**Trockenbrodt M.** 1991. Qualitative structural-changes during bark developmment in *Quercus robur, Ulmus glabra, Populus tremula* and Betula pendula. *Iawa Bulletin* **12,** 5–22.

**Van As H.** 2007. Intact plant MRI for the study of cell water relations, membrane permeability, cell-to-cell and long distance water transport. *Journal of Experimental Botany* **58,** 743–756.

**Van As H, Scheenen T, Vergeldt FJ.** 2009. MRI of intact plants. *Photosynthesis Research* **102,** 213–222.

**Williams LE, Retzlaff WA, Yang WG, Biscay PJ, Ebisuda N.** 2000. Effect of girdling on leaf gas exchange, water status, and non-structural carbohydrates of field-grown *Vitis vinifera* L. (cv. flame seedless). *American Journal of Enology and Viticulture* **51,** 49–54.

**Windt CW, Vergeldt FJ, De Jager PA, Van As H.** 2006. MRI of long-distance water transport: a comparison of the phloem and xylem flow characteristics and dynamics in poplar, castor bean, tomato and tobacco. *Plant, Cell and Environment* **29,** 1715–1729.

**Zweifel R, Item H, Häsler R.** 2000. Stem radius changes and their relation to stored water in stems of young Norway spruce trees. *Trees–Structure and Function* **15,** 50–57.

**Zweifel R, Item H, Häsler R.** 2001. Link between diurnal stem radius changes and tree water relations. *Tree Physiology* **21,** 869–877.